Colegio de Postgraduados

Synthesis of low-cost inhibitors of Spleen Tyrosine Kinase (SyK) for veterinary applications

Bello, Angélica M.[1]; Martínez-Sibaja, Albino[1*]; Landeta-Escamilla, Ofelia[1]; Vallejo-Cantú, Norma A.[1]; Méndez-Contreras, Juan M.[1]

[1] Tecnológico Nacional de México - Instituto Tecnológico de Orizaba. Orizaba, Veracruz, México. C. P. 94320.

* Correspondence: albino.ms@orizaba.tecnm.mx

ABSTRACT

Spleen tyrosine kinase (Syk) is a cytosolic enzyme that couples immune cell receptors to intracellular signaling, regulating inflammatory responses and supporting neoplastic cell survival. This study reports the synthesis of low-molecular-weight compounds with potential Syk inhibitory activity, designed as cost-effective candidates for veterinary applications.

Objective: To design, synthesize, and chemically characterize low-molecular-weight Syk inhibitors as potential anti-inflammatory and anticancer agents for veterinary use, employing a pharmacophore-based modeling strategy.

Design/Methodology/Approach: The synthetic strategy employed general pyrimidine modification protocols amenable to scale-up for pilot plant production. Blind docking simulations were conducted to estimate the interactions and binding affinities between the synthesized compounds and the Syk protein.

Results: Twenty trisubstituted pyrimidine derivatives were synthesized with yields ranging from 51% to 72%. These compounds incorporated diverse functional groups —aromatic, alkoxy, and nitrilomethylene— strategically introduced to enhance pharmacological potential while maintaining synthetic accessibility.

Limitations/Implications: This investigation was limited to laboratory-scale synthesis, chemical characterization, and blind docking analysis to estimate binding affinity. Further work is needed to optimize reaction conditions and purification protocols at the pilot-plant level to evaluate industrial scalability.

Findings/Conclusions: A total of 20 compounds bearing diverse substituents at the 2, 4, and 6 positions of the pyrimidine ring were synthesized and characterized. Notably, one compound exhibited 96% similarity in predicted binding affinity to the most potent known Syk inhibitor.

Keywords: Syk kinase, trisubstituted pyrimidine, pharmacophore modelling, veterinary therapeutics, anti-inflammatory agents.

Citation: Bello, A. M., Martínez-Sibaja, A., Landeta-Escamilla, O., Vallejo-Cantú, N. A., & Méndez-Contreras, J.M. (2025). Synthesis of low-cost inhibitors of Spleen Tyrosine Kinase (SyK) for veterinary applications. *Agro Productividad*. https://doi.org/10.32854/qs9js097

Academic Editor: Jorge Cadena Iñiguez
Associate Editor: Dra. Lucero del Mar Ruiz Posadas
Guest Editor: Daniel Alejandro Cadena Zamudio

Received: July 18, 2025.
Accepted: November 4, 2025.
Published on-line: December 11, 2025.

Agro Productividad, 18(11). November. 2025. pp: 67-80.

INTRODUCTION

Spleen tyrosine kinase (Syk) is a non-receptor cytosolic tyrosine kinase that plays a critical role in the propagation of intracellular signalling, particularly within haematopoietic cells (Mazuk *et al.*, 2008; Dauvillier *et al.*, 2002; Mócsai *et al.*, 2002). Syk has been characterized as a protein tyrosine kinase with dual oncogenic and tumour-suppressive properties (Xue *et al.*, 2012), and exhibits a unique mechanism that negatively influences cellular division.

The pivotal role of Syk in the B-cell receptor (BCR) signalling pathway underscores its relevance in tumour cell proliferation and survival. Fostamatinib disodium, a potent and selective Syk inhibitor, was the first to demonstrate promising inhibition of BCR signalling in neoplastic cells from heavily pre-treated patients with mantle cell lymphoma (Pu *et al.*, 2022). Recent studies have revealed that the loss of the long isoform (Syk-L) is associated with tumorigenesis across multiple cancer types. Notably, Syk-L serves as a substrate for Checkpoint Kinase 1 (CHK1) in tumour cells, suggesting that targeting the CHK1/Syk-L

axis may represent a promising therapeutic strategy for hepatocellular carcinoma (Hong *et al.*, 2012).

Syk also mediates immunoreceptor signalling in various cell types, including B lymphocytes, mast cells, and macrophages. Structurally, Syk comprises two Src homology 2 (SH2) domains, a linker region, and a C-terminal catalytic kinase domain. Phosphorylation of immunoreceptor tyrosine-based activation motifs (ITAMs) by upstream Src family kinases facilitates the recruitment of Syk via its N-terminal SH2 domain, resulting in its activation. Activated Syk subsequently phosphorylates downstream targets, triggering tumour cell proliferation and growth. Consequently, the inhibition of Syk by low-molecular-weight compounds presents an attractive strategy for cancer therapy (Hong *et al.*, 2012; Villaseñor *et al.*, 2009).

Given the therapeutic potential of Syk inhibitors in oncology, several pharmaceutical companies —including Novartis, Sanofi-Aventis, Boehringer Ingelheim, and GlaxoSmithKline— have expressed interest in their large-scale development.

Tyrosine kinase inhibitors (TKIs) are currently employed in veterinary oncology, particularly in canine and ovine species (Mujica *et al.*, 2021; Koltai *et al.*, 2018; Bavcar *et al.*, 2012), to target tumour cell signalling pathways and inhibit their growth and proliferation. Agents such as toceranib, masitinib, imatinib, and sunitinib are commonly used to treat various malignancies, including mast cell tumours (Álvarez *et al.*, 2012; Nakano *et al.*, 2014).

Toceranib phosphate, for instance, is a targeted therapy exhibiting both antiangiogenic and antiproliferative activity. In a multicentre clinical trial involving 151 animals diagnosed with mast cell tumours —some with regional lymph node involvement— a blinded six-week treatment phase yielded a statistically significant objective response rate of 59.5% compared to placebo. The treatment demonstrated efficacy in both mutated and non-mutated *c-kit* tumours, with higher response rates observed in the former (London *et al.*, 2012).

Despite their clinical utility, the cost of Syk inhibitors remains prohibitively high, with monthly supplies of fostamatinib reaching several thousand US dollars. This economic barrier underscores the need for the development of cost-effective Syk inhibitors for veterinary applications.

To address this challenge, a pharmacophore model for Syk was developed based on previously reported kinase inhibitors (Xie *et al.*, 2009; Villaseñor *et al.*, 2009; Atwell *et al.*, 2004). In a preliminary study, a structurally diverse set of 23 inhibitors spanning a broad activity range was selected. Common chemical features essential for potent Syk inhibition were identified. The optimal pharmacophore hypothesis comprises four key features: hydrogen bond donors/acceptors (D), hydrogen bond acceptors (A), aromatic rings (R), and hydrophobic aromatic centres (Y), along with three excluded volumes (Figure 1).

Based on this model, the synthesis of various trisubstituted structures derived from trichloropyrimidine is proposed. This preliminary study aims to evaluate the reactivity and identify optimal reaction conditions for the preparation of trisubstituted compounds bearing diverse functional groups. The initial phase involves the synthesis of derivatives incorporating hydrophobic, aromatic, and aliphatic substituents with varying polarity,

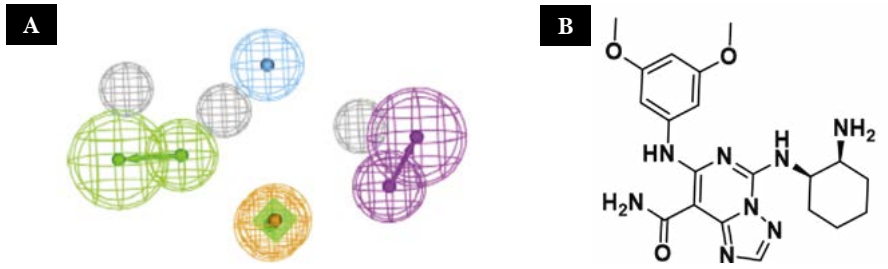

Figure 1. Pharmacophore model for spleen tyrosine kinase (Syk) inhibitors illustrating key chemical features: blue spheres represent aromatic rings, pink spheres indicate hydrogen bond donor/acceptor sites, green spheres denote hydrogen bond acceptors, and brown spheres correspond to hydrophobic aromatic centers. The chemical structure of the most potent Syk inhibitor, CHEMBL475575, is also presented for reference.

steric dimensions, and electronic density, thereby enabling a range of interactions with the target receptor. These interactions are corroborated through a Protein-ligand docking analysis using available on-line tools.

MATERIALS AND METHODS

This study comprehends two sections: synthesis of the trisubstituted compounds derived from trichloropyrimidine and docking calculations of the obtained compounds with the Syk in order to predict the inhibitory activity in comparison con compound CHEMBL475575, the most potent compound from the pharmacophore model reported (Xie *et al.*, 2009).

Potential inhibitors' Chemical Synthesis

All reagents and solvents were obtained from commercial suppliers, specifically Sigma-Aldrich and Alfa Aesar. Solvents were dried using standard procedures. Reaction progress was monitored via thin-layer chromatography (TLC), employing Merck aluminium-backed silica gel 60 plates with F254 fluorescent indicator. Purification of products was performed using column chromatography with silica gel 60 Å (70-230 mesh), applying a chloroform-methanol gradient.

Nuclear magnetic resonance (NMR) spectra were recorded on a Varian Mercury 400 MHz spectrometer for ^{1}H using deuterated chloroform ($CDCl_3$) as the solvent. Chemical shifts are reported in δ (ppm), with chloroform used as the internal reference at $\delta = 7.23$ ppm.

Monosubstituted, disubstituted, and trisubstituted derivatives of trichloropyrimidine were synthesized, incorporating substituents derived from low cost and widly available reagents such as acetonitrile, linear and branched aliphatic alcohols, and aromatic amines (Bello *et al.*, 2008). The reaction conditions do not require costly low-temperature settings, such as a -70 °C dry-ice/acetone bath for anion formation, ensuring suitability for scale-up. The synthetic pathway involves only two intermediates before obtaining the final trisubstituted pyrimidine. This relative simplicity enables lower-cost synthesis compared to molecules like CHEMBL475575, whose structural complexity —due to optically active substituents and steric hindrance— can lead to reduced yields during synthesis.

Figure 2 illustrates the synthetic pathway employed to obtain the final compounds, involving systematic substitution of trichloropyrimidine (TCP) with six different reagents: acetonitrile, aniline, anisidine, isopropanol, ethanol, and sec-butanol. This approach yielded a variety of compounds with distinct physicochemical properties depending on the order and nature of substitution. Reaction conditions, including ambient temperature and reflux, were adjusted according to the specific substituent being introduced into the pyrimidine scaffold.

Protein-ligand docking analysis

Final compounds were subjected to energy minimization by semi-empirical molecular modeling calculations utilizing the Chem3D module and the MM2 routine within ChemDraw Professional software version 18.2.1.50 (PerkinElmer, Akron, Ohio, US), before pursuing the docking protein-ligand calculations.

The docking analysis encompassed the crystal structure of ligand-free Syk retrieved from the Research Collaboratory for Structural Bioinformatics Protein Data Bank (RCSB PDB, Lee *et al.*, 2014); and the ligands consisting of 20 small pyrimidine-based compounds proposed in the present study as potential low cost Syk inhibitors. To establish a benchmark for evaluating the docking efficiency of these compounds, 5-(((1S,2S)-2-aminocyclohexyl)amino)-7-((3,5-dimethoxyphenyl)amino)-[1,2,4]-triazolo-[1,5-c]-pyrimidine-8-carboxamide (CHEMBL475575), was selected as a reference ligand based on its recognition as the most potent inhibitor from a series of compounds synthesized and characterized from the pharmacophore model (Xie e*t al.*, 2009). This analysis was conducted utilizing CB-Dock2, an advanced blind docking open-source online software application developed by Liu *et al.*, 2014. This innovative tool is designed to identify the binding regions within a protein using a curvature-based cavity detection method, which calculates the centers and dimensions of these regions to facilitate precise docking simulations. The analysis is refined by ranking the binding regions according to their Vina scores, which is a measure of the binding affinity between a ligand and a protein where more negative values indicate a stronger binding affinity. Furthermore, the software has the capacity to generate interactive 3D visualizations of the protein-ligand interactions, offering an in-depth view of the interactions between the Syk protein and the pyrimidine-based small molecules generated in the study as potential Syk inhibitors. CB-Dock2 is made publicly available at https://cadd.labshare.cn/cb-dock2/

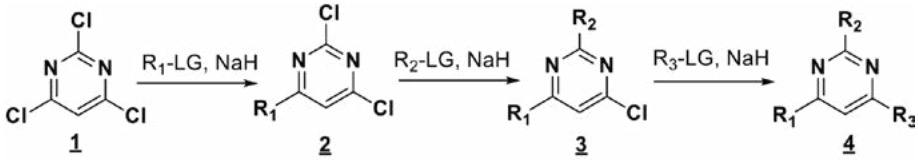

Figure 2. General reaction scheme for the synthesis of substituted pyrimidines.

index.php through the auspices of Dr. Yan Cao's Laboratory, at the College of Life Sciences, Sichuan University, China.

RESULTS AND DISCUSSION

Potential inhibitors' synthesis

Under the established reaction conditions, the interaction of trichloropyrimidine (TCP) with acetonitrile, aniline, anisidine, isopropanol, and ethanol led to the successful synthesis of five monosubstituted compounds, as illustrated in Figure 3. For alcohol-based reactions, the corresponding alcohol was used directly as the reagent. In the case of aromatic amines, anhydrous tetrahydrofuran (THF) served as the solvent. Reaction progress was monitored via thin-layer chromatography (TLC).

Crude products were purified using flash chromatography with a gradient mixture of hexane and dichloromethane as the eluent. Each compound was characterized by low-resolution mass spectrometry and proton nuclear magnetic resonance (^{1}H NMR) spectroscopy.

Seven disubstituted derivatives (3a–g) were synthesized from the previously obtained monosubstituted compounds (2a–e), using ethanol, isopropanol, and aniline as reagents, following the synthetic pathway illustrated in Figure 4. For reactions involving aniline, anhydrous tetrahydrofuran (THF) was used as the solvent. As in previous steps, reaction progress was monitored via thin-layer chromatography (TLC). Crude products were

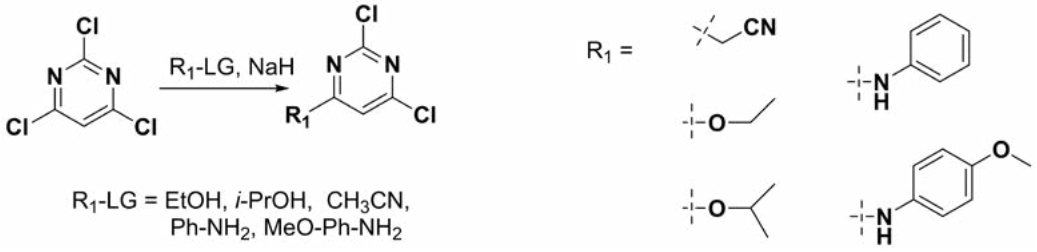

Figure 3. Synthetic scheme for monosubstituted pyrimidine compounds.

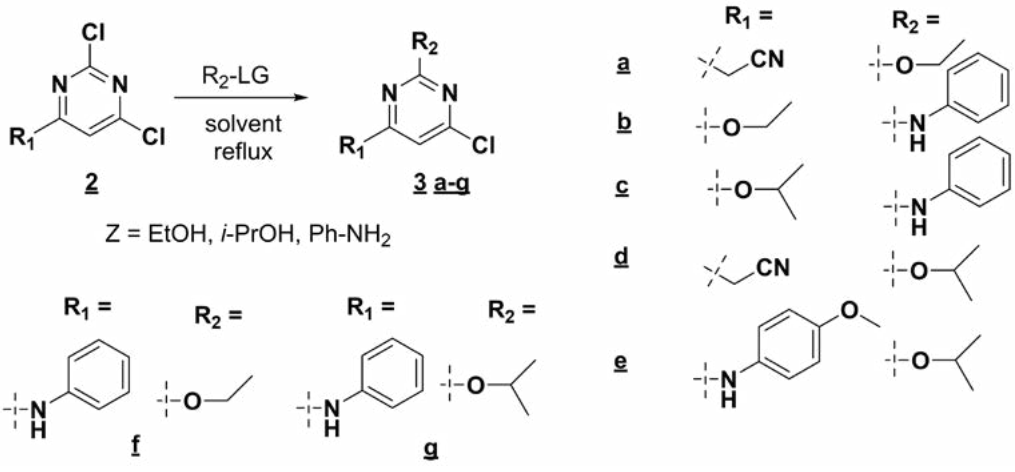

Figure 4. Synthetic scheme for disubstituted pyrimidine compounds.

purified by flash chromatography using a gradient mixture of hexane and dichloromethane as the eluent. Each compound was characterized by low-resolution mass spectrometry and proton nuclear magnetic resonance (^{1}H NMR) spectroscopy.

Additionally, twenty trisubstituted pyrimidine derivatives (4a–t) were synthesized from the disubstituted intermediates (3a–g), using ethanol, isopropanol, sec-butanol, aniline, and anisidine as reagents, following the synthetic pathway outlined in Figure 5. For reactions involving aniline and anisidine, anhydrous tetrahydrofuran (THF) was employed as the reaction solvent.

As in previous stages, reaction progress was monitored via thin-layer chromatography (TLC). Crude products were purified by flash chromatography using a gradient mixture

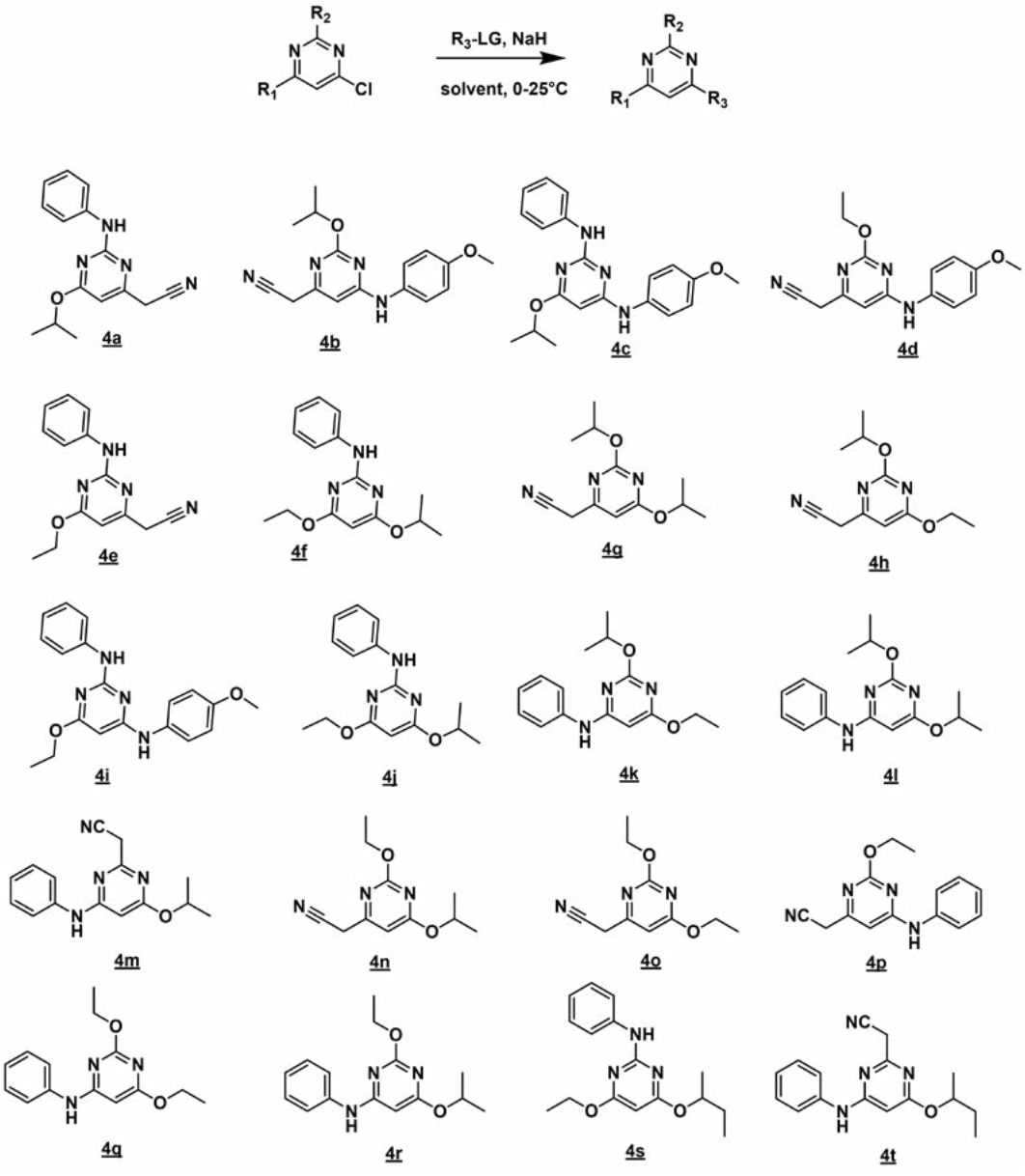

Figure 5. Synthetic scheme for trisubstituted pyrimidine compounds.

of hexane and dichloromethane as the eluent. Each compound was characterized by low-resolution mass spectrometry and proton nuclear magnetic resonance (^{1}H NMR) spectroscopy.

The initial substitution of trichloropyrimidine is governed by kinetic control at low temperature. If the reaction is allowed to proceed at ambient temperature from the outset, substitution occurs at both the 2 and 6 positions, yielding a mixture of isomers. In contrast, conducting the reaction at low temperature enables regioselective substitution at the 6-position. The substitution mechanism of trichloropyrimidine primarily follows an addition-elimination pathway.

Experimental section and characterization

In this study, from all the compounds obtained, we only describe the synthesis and characterization of three representative compounds: the monosubstituted derivative 2b, the disubstituted derivative 3c, and the trisubstituted derivative 4b.

Synthesis and Characterization of Monosubstituted Compound 2b

To synthesize the monosubstituted compound 2,4-dichloro-6-isopropoxypyrimidine (2b), sodium hydride (NaH, 60% dispersion in paraffin; 19 mg, 0.791 mmol) was weighed into a 50 mL flask under anhydrous nitrogen atmosphere and cooled to 0 °C using an ice bath. Isopropanol (65.39 mmol) was then added, and the mixture was stirred at 0 °C for 5 min. The ice bath was subsequently removed, and stirring continued at 25 °C for an additional 30 min.

The reaction mixture was then cooled again to 0 °C, and trichloropyrimidine (TCP; 150 mg, 0.094 mL, 0.817 mmol) was added. Stirring was maintained at 0 °C for 1 hour, followed by continued agitation at room temperature. Reaction progress was monitored via TLC until complete consumption of the starting material (mobile phase: hexane-chloroform 90:10).

Upon completion, the reaction was quenched with 10 mL of chloroform and 10 mL of brine. The organic layer was washed with brine (3×5 mL), dried over anhydrous sodium sulfate (Na_2SO_4), and concentrated under reduced pressure to yield the crude product. Purification was performed by flash chromatography using a dichloromethane-methanol gradient, affording compound 2b as white crystals in 83% yield (140 mg, 0.676 mmol). ^{1}H NMR for this compound is shown in Figure 6.

Synthesis and Characterization of Disubstituted Compound 3c

To synthesize the disubstituted compound 4-chloro-6-isopropoxy-2-(aminophenyl) pyrimidine (3c), a 100 mL round-bottom flask equipped with a reflux condenser was charged with compound 2b (140 mg, 0.676 mmol), aniline (90 mg, 0.088 mL, 0.966 mmol), and isopropanol (261.56 mmol). The reaction mixture was refluxed for 6 hours, with progress monitored by thin-layer chromatography (TLC) using a hexane-chloroform (80:20) mobile phase.

Upon complete consumption of the starting material, the reaction was worked up following the same protocol as for compound 2b. The crude product was purified by

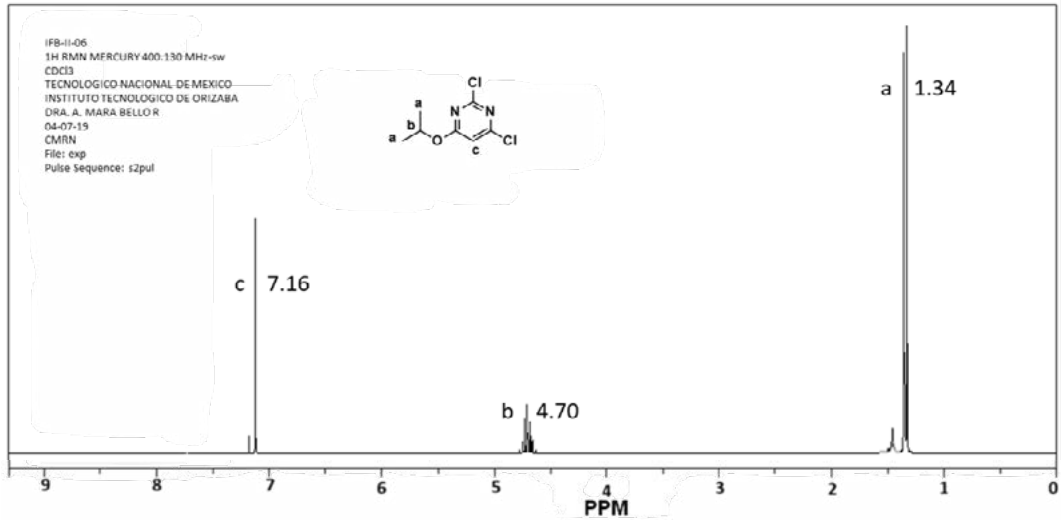

Figure 6. [1]H NMR spectra of the monosubstituted compound 2,4-dichloro-6-isopropoxypyrimidine (2b).

flash chromatography (hexane–dichloromethane gradient), yielding compound 3c as a brown solid in 67% yield (120 mg, 0.445 mmol). [1]H NMR for this compound is shown in Figure 7.

Synthesis and Characterization of Trisubstituted Compound 4b

To synthesize the trisubstituted compound 2-isopropoxy-4-(p-methoxyphenylamino)-6-(nitrilomethylene)pyrimidine (4b), sodium hydride (NaH, 60% dispersion in paraffin; 20 mg, 0.833 mmol) was weighed into a 50 mL flask under anhydrous nitrogen atmosphere and cooled to 0 °C using an ice bath. Anisidine (308 mg, 0.250 mmol) and isopropanol (261.56 mmol) were then added, and the mixture was stirred at 25 °C for 30 min.

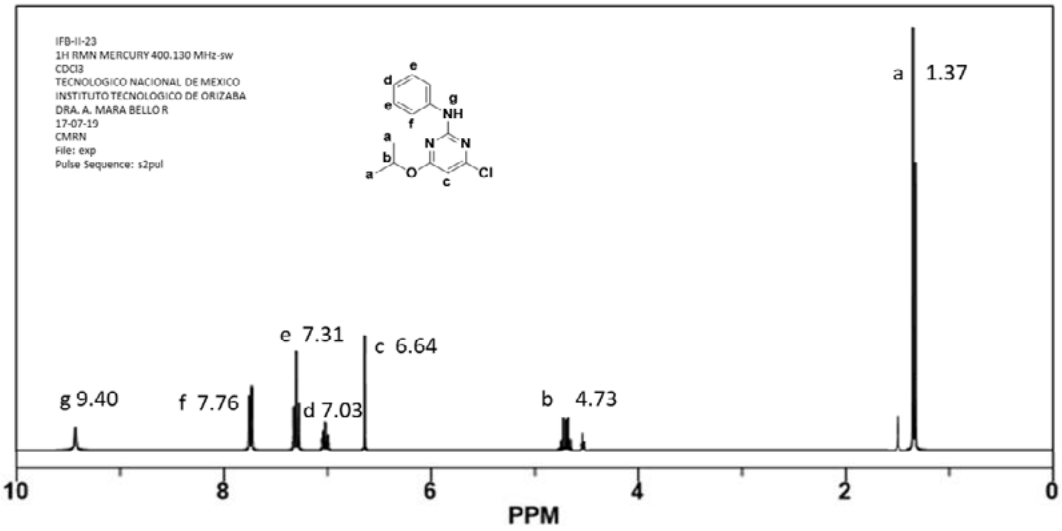

Figure 7. 1H NMR spectra of the disubstituted compound 4-chloro-6-isopropoxy-2-(aminophenyl)pyrimidine (3c).

The reaction mixture was subsequently cooled again to 0 °C, and compound 3a (1.65 mmol) was added. Stirring was maintained at 0 °C for 1 hour, followed by continued agitation at 25 °C. Reaction progress was monitored via TLC until complete consumption of the starting material (mobile phase: hexane–chloroform 90:10).

Upon completion, the reaction was quenched with 10 mL of chloroform and 10 mL of brine. The organic layer was washed with brine (3×5 mL), dried over anhydrous sodium sulfate (Na_2SO_4) and concentrated under reduced pressure to yield the crude product. Purification was performed by flash chromatography using a dichloromethane–methanol gradient, affording compound 4b as a reddish semi-liquid in 53% yield (1.17 mmol).

All the final compounds were characterized by ^{1}H NMR and mass spectrometry to establish their structure. Table 1 shows the summary of the ^{1}H NMR characterization, the low-resolution mass spectroscopy results and the yield of each of the 20 final trisubstituted compounds synthesized.

Synthesized molecules and pharmacophore model. Docking calculations

Pharmacophore model

The pharmacophore model featuring three-dimensional spatial and distance constraints employed to facilitate the design of pyrimidine-based small molecules and some of the final compounds superimposed is depicted in Figure 9. The synthesized structures fit in the pharmacophore model in at least three of the four detected features as shown in this Figure.

Docking analysis

The spleen tyrosine kinase (Syk) protein contains five distinct ligand-binding cavities. In our docking simulations, the reference inhibitor CHEMBL475575 exhibited the highest

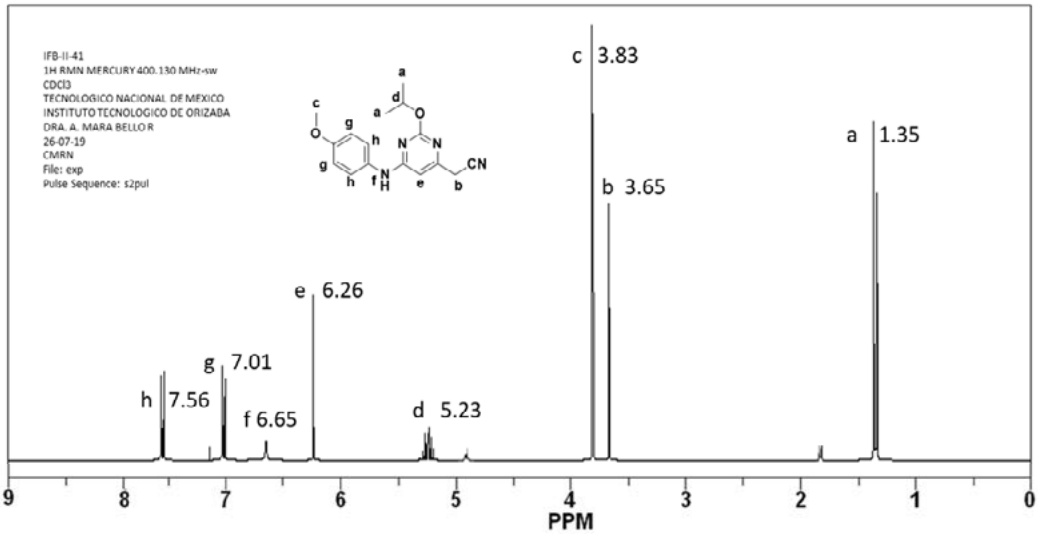

Figure 8. 1H NMR spectra of the disubstituted compound 2-isopropoxy-4-(p-methoxyphenylamino)-6-(nitrilomethylene) pyrimidine 4b.

Table 1. Characterization of trisubstituted compounds derived from TCP.

No.	RMN 1H ($CDCl_3$, δ=ppm)	m/z [MH^+] (uma)	% rend.
4a	7.72 (2H, d), 7.30 (2H, t), 6.92 (1H, t), 5.82 (1H, bs), 5.52 (1H, s), 4.71 (1H, m), 3.32 (2H, s), 1.33 (6H, d)	269.28 (enc), 269.14 (calc)	66
4b	7.53 (2H, d), 7.01 (2H, d), 6.31 (1H, s), 5.80 (1H, bs), 5.21 (1H, m), 3.81 (3H, s), 3.63 (2H, s), 1.31 (6H, d)	299.31 (enc), 299.15 (calc)	53
4c	7.72 (2H, d), 7.54 (2H, d), 7.29 (2H, t), 7.03 (2H, d), 6.91 (1H, t), 5.82 (1H, bs), 5.42 (1H, s), 4.71 (1H, m), 3.80 (3H, s), 1.32 (6H, d)	351.22 (enc), 351.18 (calc)	51
4d	7.55 (2H, d), 7.02 (2H, d), 6.24 (1H, s), 5.08 (1H, bs), 4.29 (2H, q), 3.80 (3H, s), 3.67 (2H, s), 1.29 (3H, t)	285.01 (enc), 285.14 (calc)	58
4e	7.74 (2H, d), 7.30 (2H, t), 6.92 (1H, t), 5.80 (1H, bs), 5.52 (1H, s), 4.41 (2H, q), 3.67 (2H, s), 1.36 (3H, t)	255.29 (enc), 255.12 (calc)	61
4f	7.53(2H, d), 7.29 (2H, t), 6.93 (1H, m), 5.76 (1H, bs), 5.71 (1H, s), 4.69 (1H, m), 4.40 (2H, q), 1.33 (8H, m)	274.27 (enc), 274.16 (calc)	67
4g	5.92 (1H, s), 5.31 (1H, m), 4.67 (1H, m), 3.62 (2H, s), 1.336H, d)	236.33 (enc), 236.14 (calc)	68
4h	5.92 (1H, s), 5.21 (1H, m), 4.30 (2H, q), 3.63 (2H, s), 1.33 (9H, m)	222.23 (enc), 222.12 (calc)	72
4i	7.70 (2H, d), 7.55 (2H, d), 7.28 (2H, t), 7.02 (2H, d), 6.89 (1H, t), 5.78 (2H, bs), 5.45 (1H, s), 4.38 (2H, q), 3.81 (3H, s), 1.37 (3H, t)	337.32 (enc), 337.17 (calc)	71
4j	7.71 (2H, d), 7.32 (2H, t), 6.90 (1H, t), 5.83 (1H, bs), 5.71 (1H, s), 4.70 (1H, m), 4.11 (2H, q), 1.35 (3H, t)	274.39 (enc), 274.16 (calc)	62
4k	7.53 (2H, d), 7.29 (2H, t), 6.91 (1H,, m), 5.83 (1H, s), 5.81 (1H, bs), 5.21 (1H, m), 4.39 (2H, q), 1.33 9H, m)	274.33 (enc), 274.16 (calc)	60
4l	7.53 (2H, d), 7.29 (2H, t), 6.91 (1H, t), 5.83 (1H, s), 5.80 (1H, bs), 5.21 (1H, m), 4.70 (1H, m), 1.32 (12H, d)	288.39 (enc), 288.17 (calc)	64
4m	7.54 (d, 2H), 7.31 (t, 2H), 6.91 (t, 1H), 6.02 (s, 1H), 5.89 (bs, 1H), 4.63 (m, 1H), 3.88 (s, 2H), 1.49 (d, 3H)	269.21 (enc), 269.14 (calc)	51
4n	5.94 (1H, s), 4.70 (1H, m), 4.29 (2H, q), 3.66 (2H, s), 1.34 (6H, d), 1.28 (3H, t)	222.21 (enc), 222.12 (calc)	56
4o	5.94 (1H, s), 4.41 (2H, q), 4.29 (2H, q), 3.69 (2H, s), 1.36 (3H, t), 1.27 (3H, t)	208.28 (enc) 208.11 (calc)	60
4p	7.50 (d, 2H), 7.245 (t, 2H), 6.92 (t, 1H), 6.21 (s, 1H), 5.80 (bs, 1H), 4.26 (q, 2H), 3.70 (s, 1H), 1.41 (t, 3H)	255.15 (enc), 255.12 (calc)	58
4q	7.55 (2H, d), 7.29 (2H, t), 6.90 (1H, t), 5.87 (1H, s), 5.83 (1H bs), 4.40 (2H, q), 4.26 (2H, q), 1.34 (3H, t), 1.27 (3H, t)	260.31 (enc), 260.14 (calc)	56
4r	7.51 (2H, d), 7.30 (2H, t), 6.88 (1H, t), 5.84 (1H, s), 5.82 (1H, bs), 4.72 (1H, m), 4.26 (2H, q), 1.34 (6H, d), 1.28 (3 H, t)	274.23 (enc), 274.16 (calc)	56
4s	7.79 (d, 2H), 7.26 (t, 2H), 6.80 (t, 2H), 5.73 (bs, 1H), 5.69 (s, 1H), 4.36 (q, 2H), 3.61 (m, 1H), 1.71 (m, 2H), 1.51 (d, 3H), 1.43 (t, 3H), 0.98 (t, 3H)	288.21 (enc.), 288.17 (calc)	66
4t	7.71 (d, 2H), 7.46 (t, 2H), 6.82 (t, 1H), 5.96 (s, 1H), 5.73 (bs, 1H), 3.73 (m, 1H), 3.72 (s, 2H), 1.62 (m, 2H), 1.39 (d, 2H), 0.96 (t, 3H)	283.20 (enc), 283.16 (calc)	64

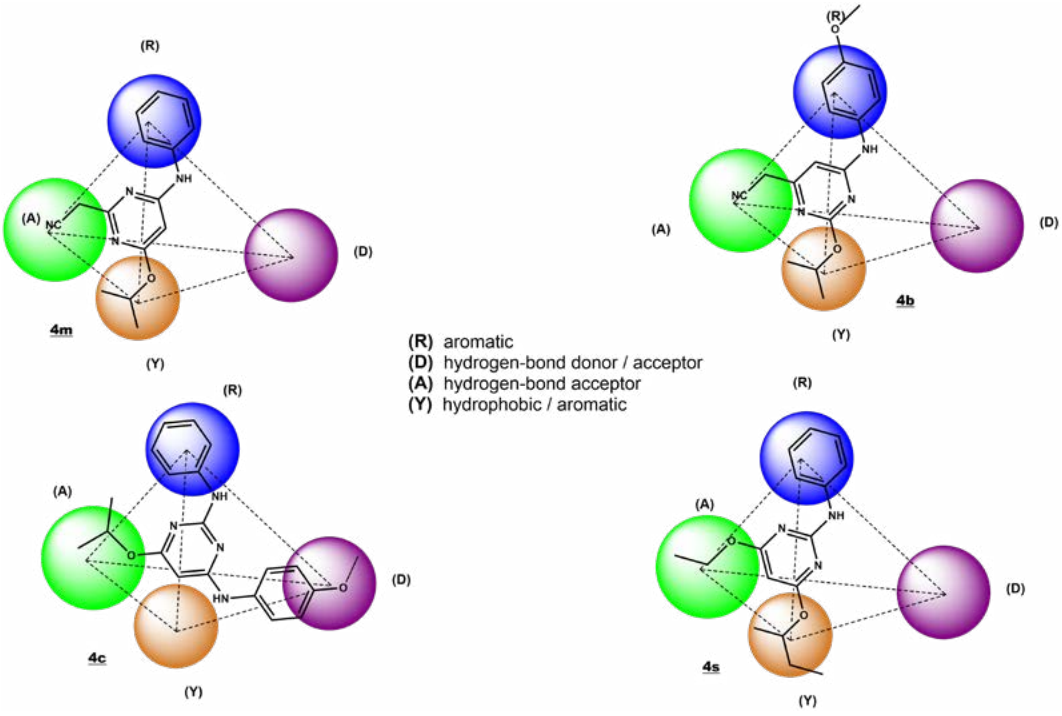

Figure 9. Trisubstituted compounds 4b, 4c, 4m and 4s superimposed into the pharmacophore model.

binding affinity for cavity 656 (volume: 656 Å^3), with a Vina score of −7.4, while the 20 pyrimidine-based compounds evaluated, showed Vina scores ranged from −7.1 to −4.8. The remaining four cavities displayed Vina scores comparable to those observed for CHEMBL475575, indicating potential alternative binding sites. Notably, the five best Vina scored synthesized pyrimidine derivatives demonstrated relatively higher docking scores within the second cavity (volume: 431 Å^3) than CHEMBL475575, as summarized in Table 2.

Qualitative analysis suggests that the macrocyclic structure of CHEMBL475575 enables it to adopt a highly favorable conformation within the Syk binding site. Its multiple aromatic rings likely promote strong $\pi-\pi$ interactions with aromatic residues, while the presence of several oxygen atoms facilitates hydrogen bonding, collectively enhancing

Table 2. Docking results (Vina score) for the 5 best compounds.

Compound	Vina Score per Pocket size In volume				
	656 Å	431 Å	398 Å	283 Å	184 Å
CHEMBL475575	−7.4	−6.4	−6.4	−7.0	−7.0
4a	−6.8	−6.6	−5.2	−5.9	−5.8
4c*	−7.1	−7.6	−5.9	−6.7	−6.6
4i*	−6.4	−7.1	−5.8	−6.2	−6.3
4m	−6.1	−6.4	−5.4	−5.5	−5.8
4t	−6.5	−6.8	−5.4	−5.7	−5.7

* The two best compounds, with the closest Vina scores to CHEMBL475575.

binding affinity. In contrast, compound ***4c***, despite containing polar functional groups (*e.g.*, ether, amine) and a heterocyclic moiety, is expected to exhibit greater conformational flexibility than CHEMBL475575. Nevertheless, its two aromatic rings may still contribute to $\pi-\pi$ interactions, partially compensating for this flexibility and improving affinity. Similarly, compound ***4i***, which ranked second in blind docking scores, underscores the importance of aromatic interactions in hotspot binding due to its two-ring structure. On the other hand, compounds ***4a***, ***4t***, and ***4m*** possess only one aromatic ring; however, the presence of a cyano group may have enhanced their binding affinities through additional polar interactions.

The interactions between the pyrimidine-based compound ***4c*** that exhibited the highest affinity (Vina score of −7.1) and the hotspot with 656Å volume was found to be 96% similar to those exhibited by CHEMBL475575 (Vina score −7.4). These interactions are illustrated in Figure 10.

The five compounds with the highest Vina scores did not exhibit the same degree of structural complexity or optimal functional group distribution as CHEMBL475575, which explains the slightly better binding interactions (*i.e.*, more negative Vina scores) observed for the reference compound. However, the relatively simpler structures and lower synthetic costs of the proposed compounds enhance their practical value, making them attractive candidates for veterinary applications.

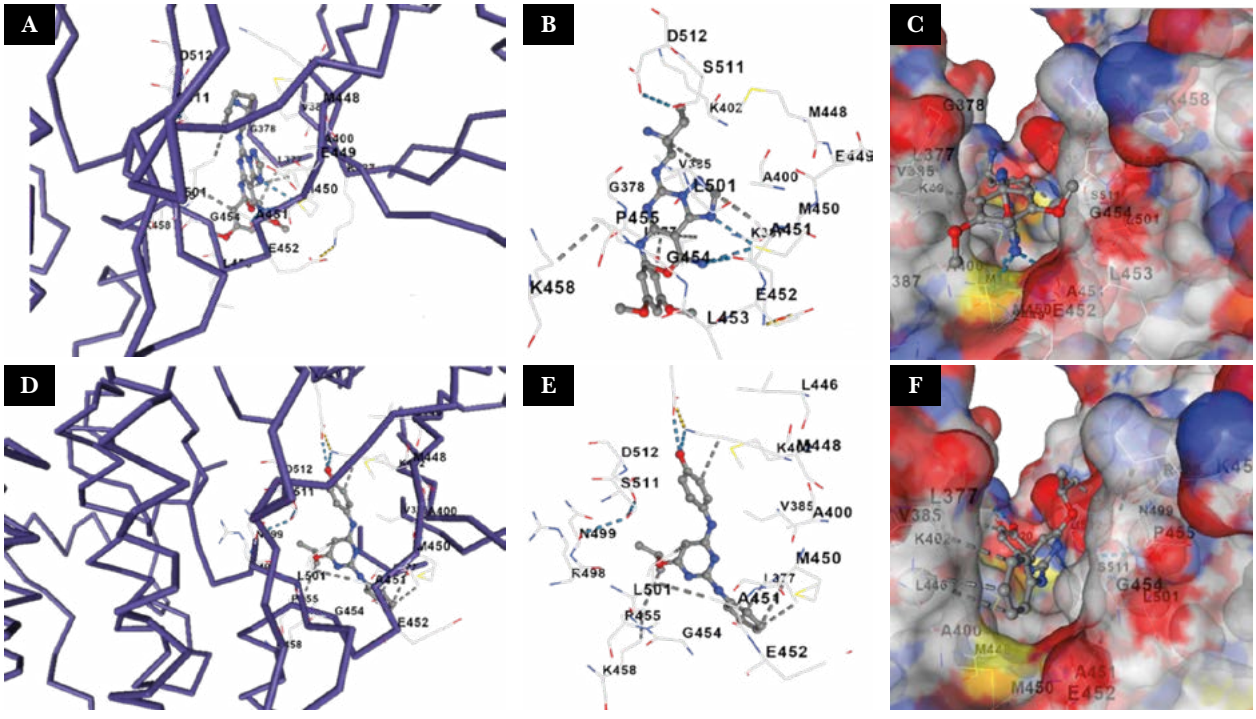

Figure 10. For CHEMBL4575575, Panels A shows the ligand bound to syk, Panel B the interactions of the ligand and de 656Å cavity and Panel C shows the protein surface and the ligand inside the cavity. Same features are shown for the synthesized compound 4c in the Panels D, E and F respectively.

CONCLUSIONS

A total of 12 intermediates derived from trichloropyrimidine and 20 final compounds bearing various substituents at the 2, 4, and 6 positions of the pyrimidine ring were successfully synthesized and characterized. The substituents exhibit diverse electronic and steric properties, including aromatic fragments, linear and branched aliphatic chains, and π-electron-rich groups. These structural features enable potential interactions with the active site of spleen tyrosine kinase (Syk), allowing the compounds to function as inhibitors at a significantly lower cost compared to commercially available drugs such as toceranib, masitinib, imatinib, and sunitinib (Álvarez *et al.*, 2012; London *et al.*, 2012; Nakano *et al.*, 2014).

The docking study confirmed the ability of the synthesized compounds to interact effectively with the Syk protein, identifying five candidates that exhibit interaction profiles comparable to those of the most potent known inhibitor. Notably, compound ***4c*** achieved a Vina score of −7.1, demonstrating approximately 96% similarity in interaction patterns with CHEMBL475575 (Vina score: −7.4).

The next phase of this research involves transforming nitrile-containing derivatives into compounds bearing amide, carboxylic acid, or primary amine functionalities. These modifications will introduce hydrophilic groups capable of forming hydrogen bonds (as donors and/or acceptors), and will also facilitate molecular extension through coupling reactions with bulkier functional groups possessing distinct physicochemical characteristics.

ETHICAL STATEMENTS

No animal testing was performed in this study

ACKNOWLEDGEMENTS

The authors gratefully acknowledge the financial support provided by the Tecnológico Nacional de México for the execution of this project (6782).18-P.

REFERENCES

Atwell, S., Adams, J.M., Badger, J., Buchanan, M.D., Feil, I.K., Froning, K.J., Gao, X., Hendle, J., Keegan, K., Leon, B.C., Müller-Dieckmann, H.J., Nienaber, V.L., Noland, B.W., Post, K., Rajashankar, K.R., Ramos, A., Russell, M., Burley, S.K., & Buchanan, S.G. (2004). A novel mode of Gleevec binding is revealed by the structure of spleen tyrosine kinase. *J. Biol. Chem*. 2004 Dec 31; 279(53): 55827-55832. doi: 10.1074/jbc.M409792200

Bavcar, S., & Argyle, D.J. (2012). Receptor tyrosine kinase inhibitors: molecularly targeted drugs for veterinary cancer therapy. *Vet Comp Oncol. 2012 Sep; 10*(3):163-73. doi: 10.1111/j.1476-5829.2012.00342.x

Bello, A.M., Bende, T., Wei, L., Wang, X., Majchrzak-Kita, B., Fish, E.N., & Kotra, L.P. (2008). De novo design of nonpeptidic compounds targeting the interactions between interferon-alpha and its cognate cell surface receptor. *J. Med. Chem. 2008 May 8; 51*(9):2734-2743. doi: 10.1021/jm701182y

Dauvillier, S., Mérida, P., Visintin, M., Cattaneo, A., Bonnerot, C., & Dariavach, P. (2002). Intracellular single-chain variable fragments directed to the Src homology 2 domains of Syk partially inhibit Fc epsilon RI signaling in the RBL-2H3 cell line. *J Immunol. 2002 Sep 1; 169*(5):2274-83. doi: 10.4049/jimmunol.169.5.2274

Hong, J., Hu, K., Yuan, Y., Sang, Y., Bu, Q., Chen, G., Yang, L., Li, B., Huang, P., Chen, D., Liang, Y., Zhang, R., Pan, J., Zeng, Y.X., & Kang, T. (2012). CHK1 targets spleen tyrosine kinase (L) for proteolysis in hepatocellular carcinoma. *J. Clin. Invest. 2012 Jun; 122*(6):2165-2175. doi: 10.1172/JCI61380

Koltai, Z., Szabó, B., Jakus, J., & Vajdovich, P. (2018). Tyrosine Kinase Expression Analyses in Canine Mammary Gland Tumours - A Pilot Study. *Acta Vet. Hung. 2018 Jun; 66*(2): 294-308. doi: 10.1556/004.2018.027

Lee, S.J., Choi, J., Han, B.G., Song, H., Koh, J.S., Lee, B.I. Research Collaboratory for Structural Bioinformatics Protein Data Bank 2014 (RCSB PDB) 4XG2 | pdb_00004xg2, URL: https://www.rcsb.org/structure/4XG2

London, C., Mathie, T., Stingle, N., Clifford, C., Haney, S., Klein, M.K., Beaver, L., Vickery, K., Vail, D.M., Hershey, B., Ettinger, S., Vaughan, A., Alvarez, F., Hillman, L., Kiselow, M., Thamm, D., Higginbotham, M.L., Gauthier, M., Krick, E., Phillips, B., Ladue, T., Jones, P., Bryan, J., Gill, V., Novasad, A., Fulton, L., Carreras, J., McNeill, C., Henry, C., & Gillings, S. (2012). Preliminary evidence for biologic activity of toceranib phosphate (Palladia®) in solid tumours. *Vet Comp Oncol. 2012 Sep;10*(3):194-205. doi: 10.1111/j.1476-5829.2011.00275.x

Mazuc, E., Villoutreix, B.O., Malbec, O., Roumier, T., Fleury, S., Leonetti, J.P., Dombrowicz, D., Daëron, M., Martineau, P., & Dariavach, P. (2008). A novel druglike spleen tyrosine kinase binder prevents anaphylactic shock when administered orally. *J Allergy Clin Immunol. 2008 Jul; 122*(1):188-194. doi: 10.1016/j.jaci.2008.04.026

Mócsai, A., Zhou, M., Meng, F., Tybulewicz, V.L., & Lowell, C.A. Syk is required for integrin signaling in neutrophils. Immunity. 2002 Apr; 16(4):547-58. doi: 10.1016/s1074-7613(02)00303-5

Mujica, P. C., Bustamante, M., Bascuñan, L., Sanhueza, V. (2021). Efectividad del tratamiento de mastocitoma cutáneo múltiple de alto grado usando un inhibidor de tirosina quinasa y vinblastina: reporte de caso. *Rev. Inv. Vet. Perú. 32*(5): 1-8. Doi: 10.15381/rivep.v32i5.16659

Nakano, Y., Kobayashi, T., Oshima, F., Fukazawa, E., Yamagami, T., Shiraishi, Y., & Takanosu, M. (2014). Imatinib responsiveness in canine mast cell tumors carrying novel mutations of c-KIT exon 11. *J Vet Med Sci. 2014 Apr; 76*(4):545-8. doi: 10.1292/jvms.13-0156

Pu, J.J., Savani, M., Huang, N., & Epner, E.M. (2022). Mantle cell lymphoma management trends and novel agents: where are we going? *Ther. Adv. Hematol.* 2022 Feb 26; 13: 1-16. doi: 10.1177/20406207221080743

Villaseñor, A.G., Kondru, R., Ho, H., Wang, S., Papp, E., Shaw, D., Barnett, J.W., Browner, M.F., & Kuglstatter, A. (2009). Structural insights for design of potent spleen tyrosine kinase inhibitors from crystallographic analysis of three inhibitor complexes. *Chem Biol Drug Des. 2009 Apr; 73*(4):466-470. doi: 10.1111/j.1747-0285.2009.00785.x

Xie, H.Z., Li, L.L., Ren, J.X., Zou, J., Yang, L., Wei, Y.Q., Yang, S.Y. (2009) Pharmacophore modeling study based on known spleen tyrosine kinase inhibitors together with virtual screening for identifying novel inhibitors. *Bioorganic Med. Chem. Lett*. 19, PP. 1944-1949. doi: 10.1016/j.bmcl.2009.02.049

Xue, L., Wang, W.H., Iliuk, A., Hu, L., Galan, J.A., Yu, S., Hans, M., Geahlen, R.L., & Tao, W.A. (2012). Sensitive kinase assay linked with phosphoproteomics for identifying direct kinase substrates. *Proc Natl Acad Sci U. S. A. 2012 Apr 10; 109*(15):5615-20. doi: 10.1073/pnas.1119418109